DECELLULARIZED LIVER BIOMATRICES AS A MODEL FOR 3D CANCER METASTASIS

An Undergraduate Research Scholars Thesis

by

HEATHER FARRIS

Submitted to the LAUNCH: Undergraduate Research office at
Texas A&M University
in partial fulfillment of requirements for the designation as an

UNDERGRADUATE RESEARCH SCHOLAR

Approved by
Faculty Research Advisor: Dr. Shreya Raghavan

May 2021

Major: Biomedical Engineering

RESEARCH COMPLIANCE CERTIFICATION

Research activities involving the use of human subjects, vertebrate animals, and/or biohazards must be reviewed and approved by the appropriate Texas A&M University regulatory research committee (i.e., IRB, IACUC, IBC) before the activity can commence. This requirement applies to activities conducted at Texas A&M and to activities conducted at non-Texas A&M facilities or institutions. In both cases, students are responsible for working with the relevant Texas A&M research compliance program to ensure and document that all Texas A&M compliance obligations are met before the study begins.

I, Heather Farris, certify that all research compliance requirements related to this Undergraduate Research Scholars thesis have been addressed with my Research Faculty Advisor prior to the collection of any data used in this final thesis submission.

This project required approval from the Texas A&M University Research Compliance & Biosafety office.

TAMU IBC #: 2020-004 Approval Date: 03/30/2020 Expiration Date: 03/30/2023

TABLE OF CONTENTS

ABSTRACT

Decellularized Liver Biomatrices as a Model for 3D Cancer Metastasis

Heather Farris
Department of Biomedical Engineering
Texas A&M University

Research Faculty Advisor: Dr. Shreya Raghavan
Department of Biomedical Engineering
Texas A&M University

Ovarian cancer is metastatic at the time of diagnosis, with the liver being one of the most common sites of metastasis. Infiltrative liver metastases are not amenable to optimal surgical removal; moreover, liver metastases are resistant to chemotherapy. Importantly, cancer cells interact with the immune microenvironment in metastatic organs to establish metastatic colonies. Specifically, macrophages are responsible for increased infiltration of cancer cells. Therefore, new forms of nano-immunotherapy can be utilized to target the interaction between macrophages and cancer cells. Conventional metastasis and cell invasion assays do not recapitulate the native primary or metastatic tumor microenvironments, and hence, do not predict drug efficacy very well. Decellularized liver biomatrices are an attractive alternative for in vitro drug screening to provide a more accurate 3D model of the metastatic microenvironment. Liver biomatrices were manufactured via sectioning and decellularization with a Triton X-100 and Ammonium Hydroxide detergent solution. The decellularized liver biomatrices were evaluated using scanning electron microscopy (SEM), DNA quantification, and histology to verify that the native cells had been successfully removed. Ovarian cancer cell (OVCAR 3) spheroids were then

cultured with and without macrophages on hanging drop arrays and seeded onto the biomatrices to simulate metastasis. Samples were harvested at various timepoints in order to study the influence of macrophages on the invasive properties of metastatic ovarian cancer cells. Fixed biomatrices were imaged using scanning electron microscopy then analyzed with ImageJ software to quantify and compare ovarian cancer cell invasion across the different conditions. Preliminary SEM and histology data confirm adequate decellularization of the liver tissue. Therefore, the decellularized liver biomatrix can be used as a 3D model of the hepatic tumor microenvironment for the study of nano-immunotherapies for ovarian cancer liver metastasis (OCLM) as well as other forms of liver metastasis.

ACKNOWLEDGEMENTS

Contributors

I would like to thank my faculty advisor, Dr. Shreya Raghavan, for the opportunity to do this research and work in her lab. Additionally, I thank Dr. Biswajit Saha and Sabrina VandenHeuvel for their guidance and support throughout the course of this research.
I want to extend my appreciation to my colleagues and the Biomedical Engineering department faculty and staff for making my time at Texas A&M University a great experience thus far. Finally, I want to thank my friends and family for their encouragement.

I would like to acknowledge Sabrina VandenHeuvel for her work with cell culture and biomatrix seeding for this project. Also, Amanda Myatt and Dr. Holly Gibbs and the Microscopy and Imaging Center kindly trained and assisted me on sample processing and imaging equipment necessary for the completion of this project. Figures were created in part with BioRender.com.

All other work conducted for the thesis was completed by the student independently.

Funding Sources

This work was supported by the Texas A&M Engineering Experiment Station and the Texas A&M Department of Biomedical Engineering. This work was additionally supported by the Houston Methodist Cancer Center Innovation Award through the Kaplan Gynecologic Cancer Fund (SR).

NOMENCLATURE

OCLM	Ovarian Cancer Liver Metastasis
DI	Deionized
ECM	Extracellular Matrix
SEM	Scanning Electron Microscopy
TME	Tumor Microenvironment
TAM	Tumor-associated Macrophage
OVCAR	Ovarian Carcinoma
PFA	Paraformaldehyde
TDF	Tumor-derived Factors
CSC	Cancer Stem Cell

1. INTRODUCTION

1.1 Ovarian Cancer Liver Metastasis

1.1.1 Motivation

Ovarian cancer is the fifth highest in cancer deaths among women; it is estimated 13,770 women will die of it in 2021 [1]. This is likely due to the fact that ovarian cancer has subtle symptoms and currently there is no accurate screening test for it. Most patients are diagnosed with advanced stage ovarian cancer that is more likely to be metastatic than if it had been found sooner [1]. In the United States, the average lifetime risk for a woman to develop ovarian cancer is 1.3% and less than half of those diagnosed will live more than 5 years post diagnosis [2]. The 5 year survival rate significantly decreases for stage 4 ovarian cancer [2].

The liver is a common target organ for ovarian cancer metastasis; in one study on the patterns in serous ovarian cancer it was found that 34% of the patients with serous ovarian cancer developed hepatic involvement [3]. Metastasis in the liver is unique in that it uses the liver's existing vasculature rather than modifying the structure [4]. This causes problems for common cancer treatments because the lower level of vascularization within the tumor decreases the efficacy of high molecular weight therapies [4]. Additionally, high levels of liver metastasis create difficult conditions where surgeons are unable to resect the tumors leading to limited patient survival.

Macrophages are present in large quantities in the peritoneal ascites and interact with the cancer stem cells (CSCs) in the tumor microenvironment (TME) [5]. Additionally, cancer metastasis and recurrence are influenced by the activation of macrophages by tumor-derived factors (TDFs) [5]. It is important to further evaluate the effects of interactions between ovarian

cancer cells and macrophages on cancer metastasis for future OCLM therapies targeting macrophages.

1.1.2 Current Treatments

The current standard treatment for OCLM is liver resection and chemotherapy. Optimal debulking is the primary treatment option, but the tumor cannot be fully removed in cases with high liver metastasis. When optimal debulking cannot be carried out, there is a decrease in patient survival. These treatments are invasive and can cause harsh side effects for the patient. Additionally, chemotherapy has been found to be unsuccessful as a treatment for liver metastasis and for attaining sustained remission [4, 6]. Thus, a targeted immunotherapy could be beneficial for the patients' well-being and improve survival rate.

1.2 Macrophages

Macrophages are a component of the innate immune system that are phagocytic and engulf foreign particles and bacteria in the body [4]. Macrophages are found in large quantities within the peritoneal ascites; these macrophages interact with cancer stem cells (CSCs) and TDFs within the TME and influence cancer metastasis and tumor growth [4, 5].

Tumor activity can either be supported or inhibited depending on the phenotype of the macrophage. Macrophages can be pro-inflammatory, M1, and inhibit tumor growth through the secretion of pro-inflammatory cytokines, or anti-inflammatory, M2, and support tumor growth through the secretion of anti-inflammatory cytokines and growth factors [4]. The macrophages in the peritoneal ascites are heterogeneous, so both phenotypes are present. The ratio of M1:M2 is a determining factor for liver metastasis prognosis; a high ratio is associated with a better prognosis than a low ratio [4, 5]. A lower ratio of M1:M2 is also associated with cancer recurrence and cancer cell proliferation after treatment [4]. Interactions between the tumor cells

and macrophages influence the cancer growth in the liver. The TDFs in the liver TME can polarize macrophages to the M2 phenotype [5]. For example, tumor-derived cytokines and chemokines activate macrophages to tumor associated macrophages (TAMs).

1.3 Hepatic Tumor Microenvironment

The hepatic tumor microenvironment affects the tumor's growth, proliferation, and survival in the body. The liver extracellular matrix (ECM) plays an important role in cancer metastasis [7]. The ECM is composed of fibrous proteins and proteoglycans [8]. The most abundant protein in the ECM is collagen; increased collagen density in TMEs has been associated with an increase in cancer cell invasion and tumor progression [8]. The ECM can be remodeled by the cancer cells to create a microenvironment more suitable for tumor cell survival [8]. Other proteins of the ECM also influence the TME, such as fibronectin, tenascin, and laminin [8]. These acellular components of the ECM can increase the tumor growth and can be evaluated through the use of decellularized biomatrices that maintain the liver ECM.

Additionally, cells within the TME interact with the tumor cells and can have both positive and negative effects on the tumor's survival [4]. Macrophages are found in large quantities within the liver TME [5]. As stated earlier, the interactions between native macrophages in the liver TME and TDFs are important factors for cancer metastasis.

1.4 Modeling the Hepatic Tumor Microenvironment

1.4.1 Conventional Metastasis Models

Traditional models for metastasis have been used to research cancer cell behavior and drug efficacy for decades, but these conventional models have their limitations.

A common model is scratch or wound healing; this method has the benefit of being highly accessible and simple to analyze cell migration by distance and speed [9]. In wound

healing assays, cells are seeded on a tissue culture plate and a pin is used to make a thin uniform 'scratch' through the cell monolayer [9, 10]. The wound is then observed at set time points and the decreasing width of the induced wound is measured to quantify cell migration [9]. Common limitations of wound healing assays are high variability, poor reproducibility, and a lack of complexity that is found in the ECM that influences cell migration [10].

Another model is the Transwell cell invasion assay which is used to evaluate invasion through the ECM and chemotaxis [9]. A Transwell membrane is used as a physical membrane that cells travel through towards a chemo-attractant [9]. The cell migration can be evaluated through the use of time lapse or live cell imaging [9]. Evaluation of this model can be complicated with conventional microscopy and it is difficult to get significant results from testing [9, 10].

The Transwell assay can be improved for ECM evaluation with the addition of Matrigel to the surface of the Transwell membrane [9, 10]. Matrigel is a natural ECM-based hydrogel that contains ECM membrane proteins and growth factors [11]. The addition of the Matrigel increases the effectivity of the model to evaluate cell invasion and mimic the conditions of the native ECM [11]. Matrigel assays do have limitations associated with them, such as difficulties with assay setup and maintaining concentration gradients throughout the experiment, cell motion cannot be observed until the completion of the experiment, and cells must migrate through a synthetic polymer filter [12].

Another conventional metastasis model is in vivo rodent models. These models can be easily scaled up and are more similar biologically to the human liver TME than 2D in vitro cultures. However, rodent models also have drawbacks, such as ethical concerns with the use of animals, high cost, extended timeline for results, and biological differences between rodents and

humans [13]. The decellularized liver biomatrix can be used as an alternative to these conventional metastasis models to overcome the limitations stated above and increase the accuracy of in vitro drug efficacy results.

1.4.2 Decellularized Liver Biomatrix

The decellularized biomatrix is another option for modeling the liver TME in vitro. When producing the decellularized liver biomatrix, there are two main options: whole organ and partial liver decellularization. Whole organ decellularization is often used for the purpose of transplantation and regenerative medicine [14]. The liver biomatrices in this experiment are being made for the purpose of modeling the TME for the in vitro testing of OCLM nano-immunotherapy. For this reason, the liver biomatrices are made out of small sections of the liver.

For in vitro cancer treatment research, it has been found that 3D cultures more accurately represent the TME than 2D cultures do because the cancer cells have different morphologies and growth within each method [15]. Additional benefits to the liver biomatrix are that the ECM of the liver and the bioactivity and growth factors are preserved in the decellularization process [4].

Decellularized liver biomatrices can be engineered to research specific stages and conditions of metastasis [4]. In this case, the impact of macrophages on ovarian cancer cell morphology and proliferation is investigated. However, this strategy can be applied to study other cells or microenvironments in the liver TME.

1.4.3 Spheroids

Spheroids are a 3D spherical organization of multiple cancer cells that can be supported using a gel or scaffold [4, 6]. Hanging drop array platforms can be used to form spheroids with high circularity and a variety of cancer cell volumes [6]. Specific conditions can be studied through the engineering of spheroids with varying ECM molecules [4, 6]. For example, in this

project, the influence of macrophages on ovarian cancer metastasis potential is studied through the use of spheroids created to contain both ovarian cancer cells and macrophages [5]. The influence of macrophages on the ovarian cancer cell proliferation can then be determined by comparing ovarian cancer monospheroids to ovarian cancer cells and macrophages cultured together in heterospheroids. A benefit to the spheroid model is the ability to investigate the cell-cell interactions in a 3D environment where cell morphologies and growth kinetics more accurately represent that of the true TME. [5]. Spheroids can be used in conjunction with other metastasis models to increase the accuracy of the model.

Spheroids are particularly beneficial for studying OCLM [6]. Ovarian cancer cells are known to naturally grow and organize as spheroids in the peritoneal fluid (ascites) during metastasis [4, 6]. Additionally, the use of spheroids can increase the accuracy of drug efficacy results for in vitro testing when compared to in vivo outcomes. Cancer spheroids tend to have a lower proliferation rate and higher chemoresistance than cancer cells in 2D cultures; this is more similar to results from in vivo tumors [6]. Spheroids increase the accuracy of the in vitro TME model as well as allow for studying specific cell interactions within the TME.

1.5 Future Impact

Current research is focused on targeted immunotherapies and immunosuppression of tumor-associated macrophages, tumor-infiltrating T cells, and tumor-associated dendritic cells [16]. The macrophages in the TME can be targeted for cancer nano-immunotherapy because the macrophages will take up the drug particles in circulation [4]. Targeting TAMs is most commonly accomplished by transforming macrophages from M2 to M1 [17]. This increases the M1:M2 ratio and, thus, may result in an improved prognosis. Alternatively, TAMs can be harnessed for drug delivery [17]. Depending on which strategy is chosen and the type of cancer,

the immunotherapies will differ. Benefits of nanotherapies over conventional cancer therapies are that drug concentrations can be increased, the drugs spend a longer time in circulation, and the drug release can be controlled and specifically targeted [4]. One common issue with immunotherapies for cancer treatment is that the tumor microenvironment is very complex, so it can be difficult to elicit a consistent and specific response in each patient [17]. Through the use of the liver biomatrix model, nano-immunotherapies for OCLM can be tested for drug efficacy in a more accurate model of the tumor microenvironment.

2. METHODS

2.1 Research Objectives

1. Decellularize porcine liver
2. Characterize decellularization of biomatrix
3. Culture ovarian cancer cell spheroids
4. Introduce ovarian cancer cell spheroids to liver biomatrix
5. Analyze and quantify invasion of cancer cells into the biomatrix

2.2 Liver Biomatrix Decellularization

Porcine livers were collected fresh and stored at -80°C for use in this experiment (Jarett's Meat Services, Madisonville, Texas). The porcine liver was cut into disks around 5 mm thick as shown in Figure 2.1-A. Decellularization was accomplished through a multi-day rinsing process involving DI water and a detergent solution. The detergent solution consisted of Triton X-100 (0.1%) and 20% Ammonium Hydroxide (0.01%) in DI water. The samples were rinsed with DI water for 3 days, then with detergent solution for 3 days, and finally with DI water for another 3 days. The samples were constantly rotated and stored at 4°C during the entirety of the rinsing process. An image of a liver biomatrix sample following the first water rinse is shown in Figure 2.1-B and the results of the detergent rinse are shown in Figure 2.1-C. The decellularized liver samples were lyophilized for 48 hours following the rinsing procedure. The final, lyophilized liver biomatrix is shown in Figure 2.1-D.

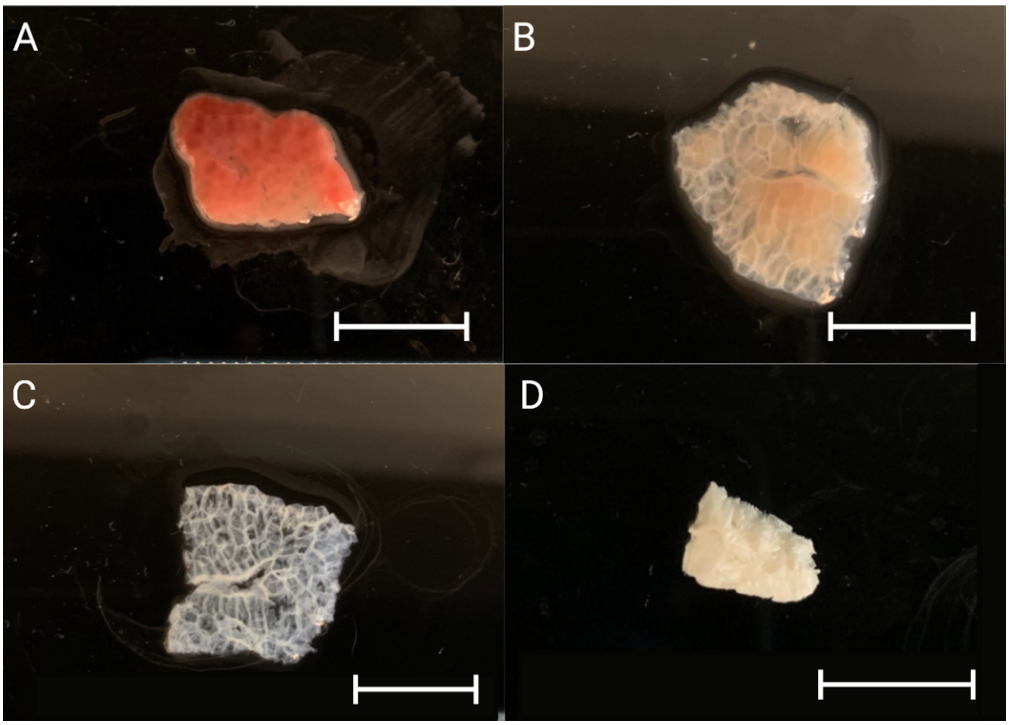

Figure 2.1: The progression of liver decellularization: A) fresh porcine liver after resection, B) liver sample after 3 days water rinse, C) liver sample after 3 days of detergent rinse, and D) final lyophilized liver biomatrix. Scale bar in each picture represents 1 cm.

2.3 Characterization of Decellularized Biomatrix

The decellularization of the liver biomatrix had to be characterized to determine the efficacy of the decellularization process. This was accomplished using multiple methods: histology, SEM, and DNA isolation and quantification.

2.3.1 Histology

Histological evaluation of the liver biomatrix was performed to confirm decellularization. Slide preparation was performed by the Texas A&M CVM Histology lab. The slides were stained with H&E and DAPI. Hematoxylin and Eosin, also known as H&E, is a stain commonly used for viewing cell structure [18]. H&E is used in this project to show the ECM structure left

after the decellularization process and to confirm the absence of nuclei. The H&E-stained slides were imaged using a Leica microscope with brightfield illumination.

DAPI or 4',6-diamidino-2-phenylindole is a blue-fluorescent DNA stain that binds to AT regions of DNA [19]. This causes the nucleus to glow blue if DNA is present. The decellularized liver biomatrix is expected to have no DNA present, so there should be no bright blue spots visible. The DAPI stained slides were imaged using a Leica microscope with fluorescent illumination at 405nm.

2.3.2 Scanning Electron Microscopy (SEM)

The decellularized liver biomatrix samples were dried using a lyophilizer. The biomatrix was cut approximately half-way through to show the cross-section of the sample. The samples were then processed using the Sputter Coater Ted Pella Cressington 108 which coated the surface and the cross-section faces of the sample in a conductive layer of gold. The Scanning Electron Microscope JEOL JCM-5000 NeoScope was then used to image the samples. The samples were analyzed from two different orientations (longitudinal and transverse) and the entirety of the sample was examined in multiple magnifications.

2.3.3 DNA Quantification

The QIAamp DNA Micro Kit from Qiagen was used in order to quantify the amount of DNA remaining in the decellularized biomatrix compared to the fresh liver samples, following manufacturer protocols. Fresh liver samples were transected and lyophilized for 2 days prior to DNA extraction. Dry weight of the liver biomatrices and fresh liver samples were measured prior to DNA extraction. The NanoDrop OneC was used to quantify the DNA content of the samples. Each sample was tested 10 times and the results were averaged for each and normalized to tissue weight.

2.4 Ovarian Cancer Spheroid Culture

2.4.1 Spheroid Generation

OVCAR 3 cells (human high grade serous ovarian carcinoma cell lines) were cultured and treated with trypsin per a regular passage. Cells were collected and plated on 384-well hanging drop spheroid arrays using protocols established previously [5, 6]. OVCAR 3 cells were allowed to aggregate and form spheroids over 4 days; upon which, they were harvested from hanging drop array plates and seeded onto decellularized liver biomatrices.

Heterospheroids were generated by combining OVCAR 3 cells and THP-1 (monocyte cell line)-derived macrophages. THP-1 macrophages were derived using phorbol ester treatment for 72 hours, following which a 1:1 ratio of macrophages and OVCAR 3 cells were combined and plated into hanging drop array plates [5]. Heterospheroids were seeded, following 4 days of culture, onto liver biomatrices.

2.4.2 Preparation of Biomatrix and seeding of Metastatic nests

The biomatrices were cut to approximately 0.5 mg sections, weighed, and saturated with FBS. Individual biomatrices were then attached to Sylgard-coated 24 well plates with the use of insect pins. The spheroids were seeded onto the biomatrix with 20 spheroids per 0.5 mg of biomatrix. The spheroids were allowed to grow for 3 to 7 days before fixation with 4% paraformaldehyde (PFA).

2.5 Quantification of Cell Invasion

2.5.1 Scanning Electron Microscopy

The recellularized liver biomatrix samples containing the spheroids were lyophilized and cut approximately halfway through the sample. The sample was then processed using the Sputter Coater Ted Pella Cressington 108 which coated the surface and cross-section of the sample in a

conductive layer of gold. The Scanning Electron Microscope JEOL JCM-5000 NeoScope was then used to image the samples. The samples were analyzed from different magnifications and the entirety of the sample was examined. Multiple images were taken for each day of growth analyzed. Typical timepoints analyzed included days 3, 5, and 7 following recellularization.

2.5.1.1 Cell Area Quantification

SEM images showing mono- and heterospheroid occupation of the biomatrix were used to quantify cell invasion. ImageJ software was applied for quantification using the same image processing parameters for each image to ensure consistency. First, the image was scaled based on the scale bar dimensions and the brightness, contrast, and sharpness were adjusted to increase image clarity. Cell area borders were traced and filled in using the freehand tool. The image threshold was then adjusted so that the cell area appeared red and the background was excluded by the threshold. The image was converted to a binary mask and the noise removed. This process is shown in Figure 2.2. The measurements were set to area, standard deviation, and area fraction and limited to threshold. All results were exported as Microsoft Excel files. OVCAR 3 monospheroids and OVCAR 3/macrophage heterospheroids were analyzed on days 3 and 7 of growth. For each of these categories, 3 images were quantified using ImageJ.

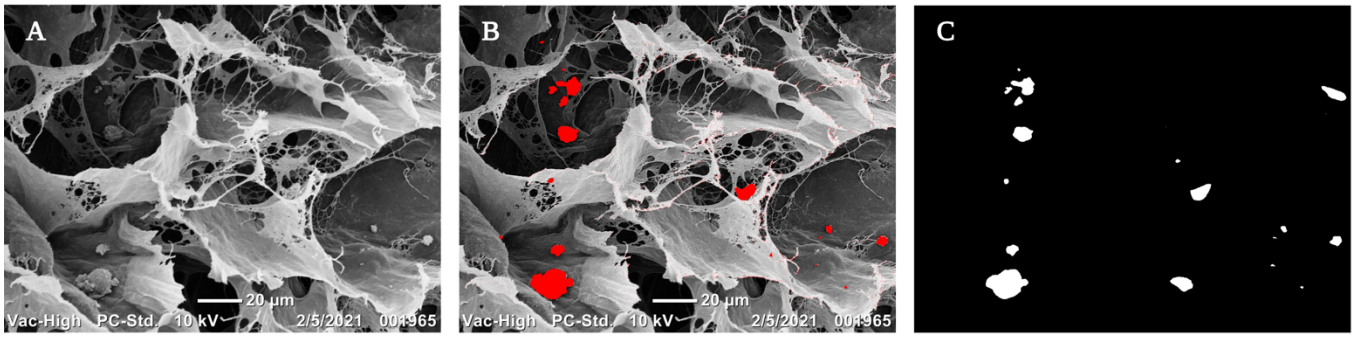

Figure 2.2: Stepwise ImageJ image analysis for cell quantification – A) original SEM image, B) SEM image after thresholding showing cell clusters in red, C) binary mask of the threshold image used for cell area quantification

The mean and standard deviation for percent cell area were calculated for each timepoint. Statistical significance was determined with a one-way ANOVA conducted using GraphPad Prism software.

3. RESULTS

Results Overview:

1. Liver Biomatrix Decellularization
2. Spheroid Imaging
3. Spheroid Cell Quantification

3.1 Liver Decellularization

The decellularization of the liver biomatrix had to be proven effective before moving forward to use it as a metastasis model. This was accomplished through three characterization methods: histology, SEM, and DNA quantification, the results of which are shown below.

3.1.1 Histology Results

The results of the DAPI staining on the decellularized liver biomatrix are shown in Figure 3.1. The nuclei of the cells would glow bright blue if DNA was present. Nuclei were not visible during imaging indicating that the DNA content has been cleared from the sample.

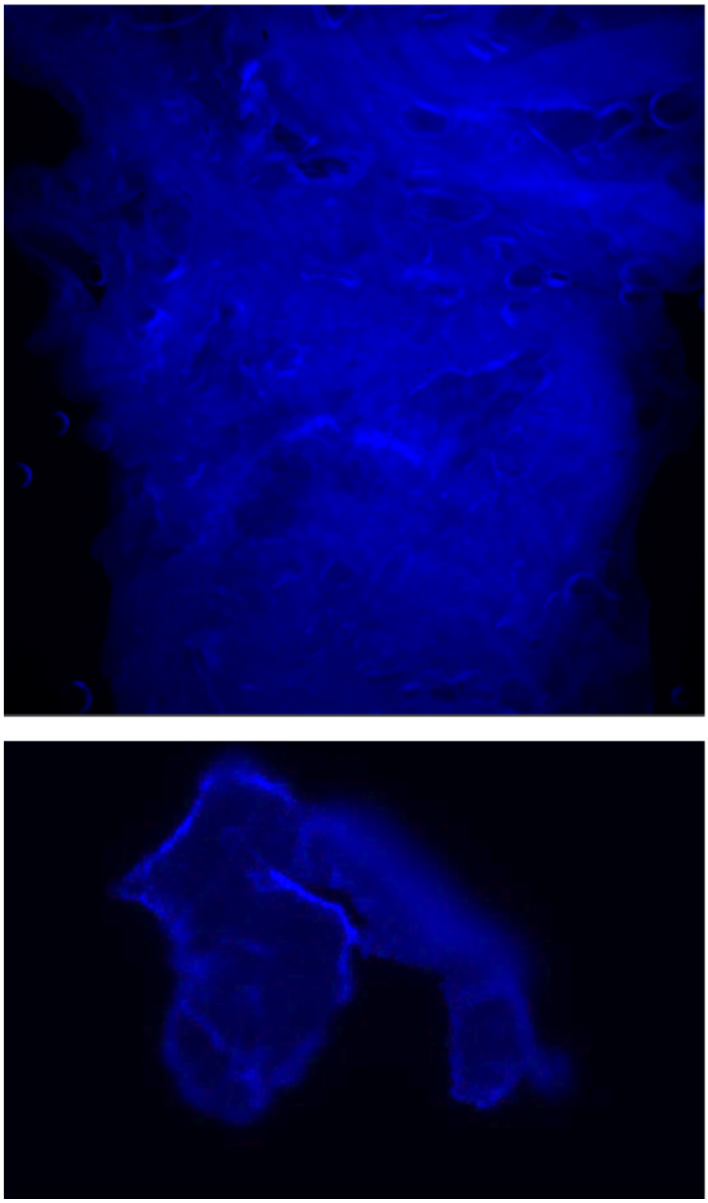

Figure 3.1: DAPI stained decellularized liver biomatrix histology slides from two different samples

The results from H&E staining on the decellularized liver biomatrix are shown below in Figure 3.2. The image shows the decellularization of the decellularized liver biomatrix compared to a biomatrix containing OVCA cells.

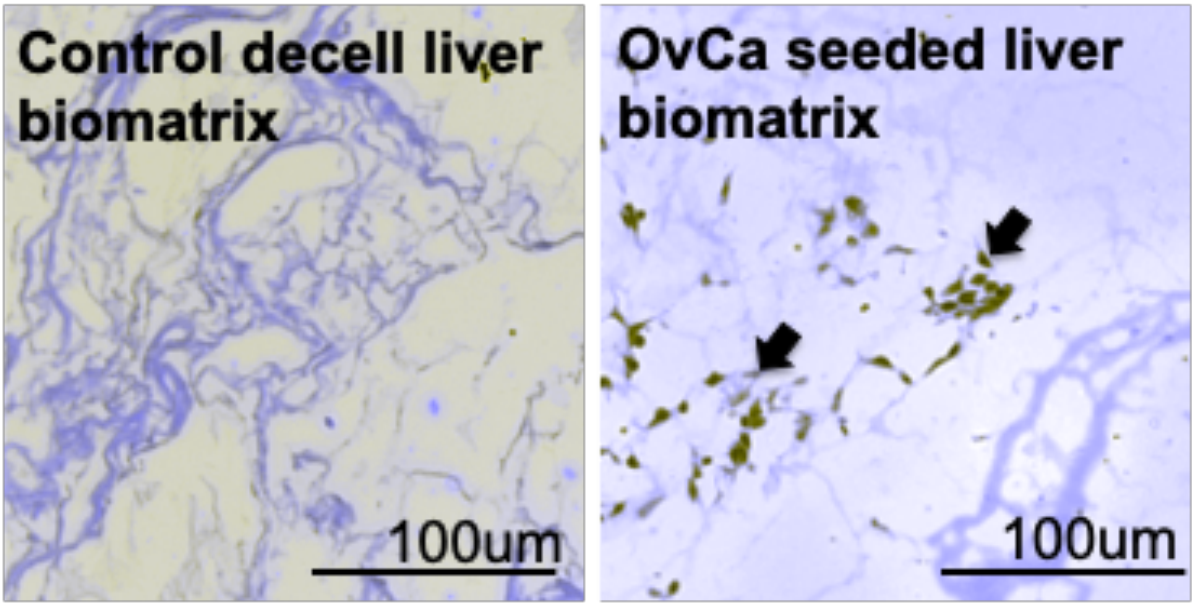

Figure 3.2: H&E stained decellularized liver biomatrix (left) and OVCA seeded liver biomatrix (right) imaged with brightfield illumination. Arrows indicate OVCA cell nuclei.

3.1.2 Scanning Electron Microscopy Images

SEM was used to visually confirm the absence of native cells in the decellularized liver biomatrices. SEM images were taken of fresh liver samples as a control at a low and high magnification. These images are shown below in Figure 3.3.

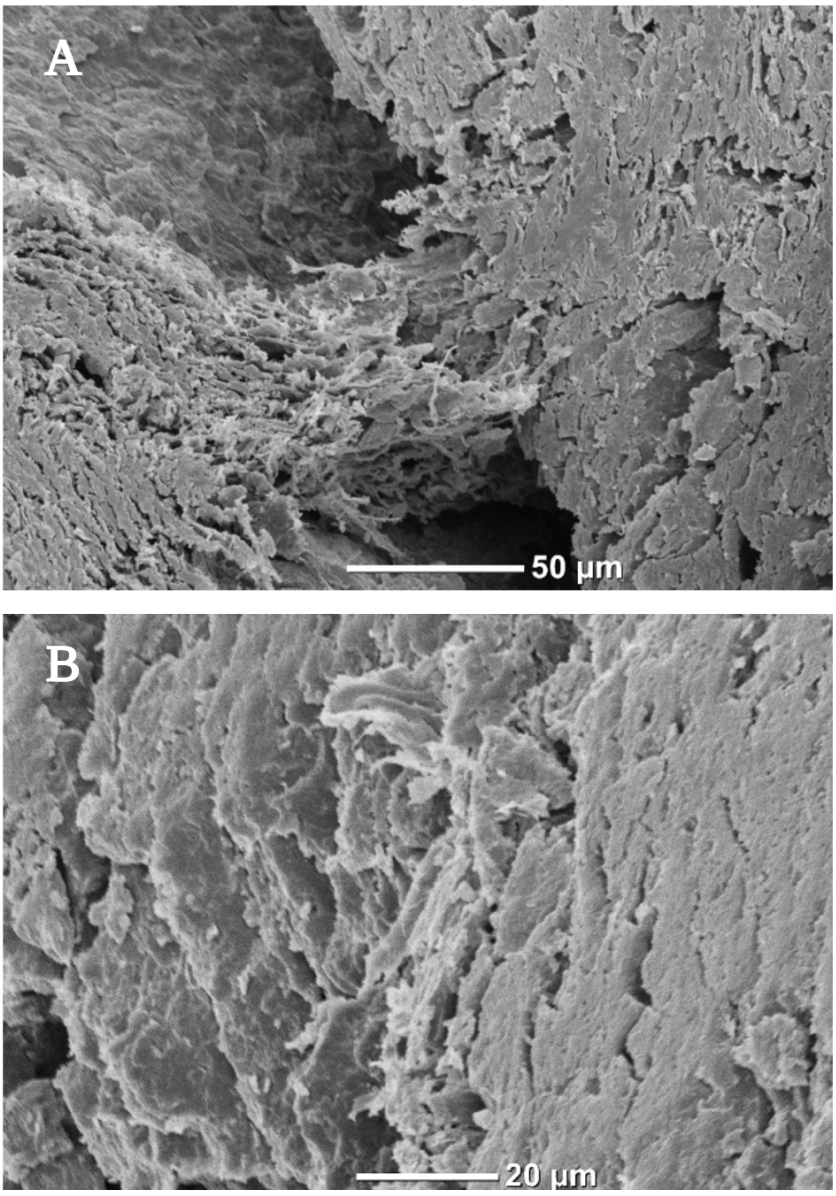

Figure 3.3: SEM images of fresh liver samples at A) 500x and B) 1000x magnification

The images in Figure 3.4 below show the decellularized liver biomatrix at a high and low magnification. Both magnifications show the absence of visible native cells.

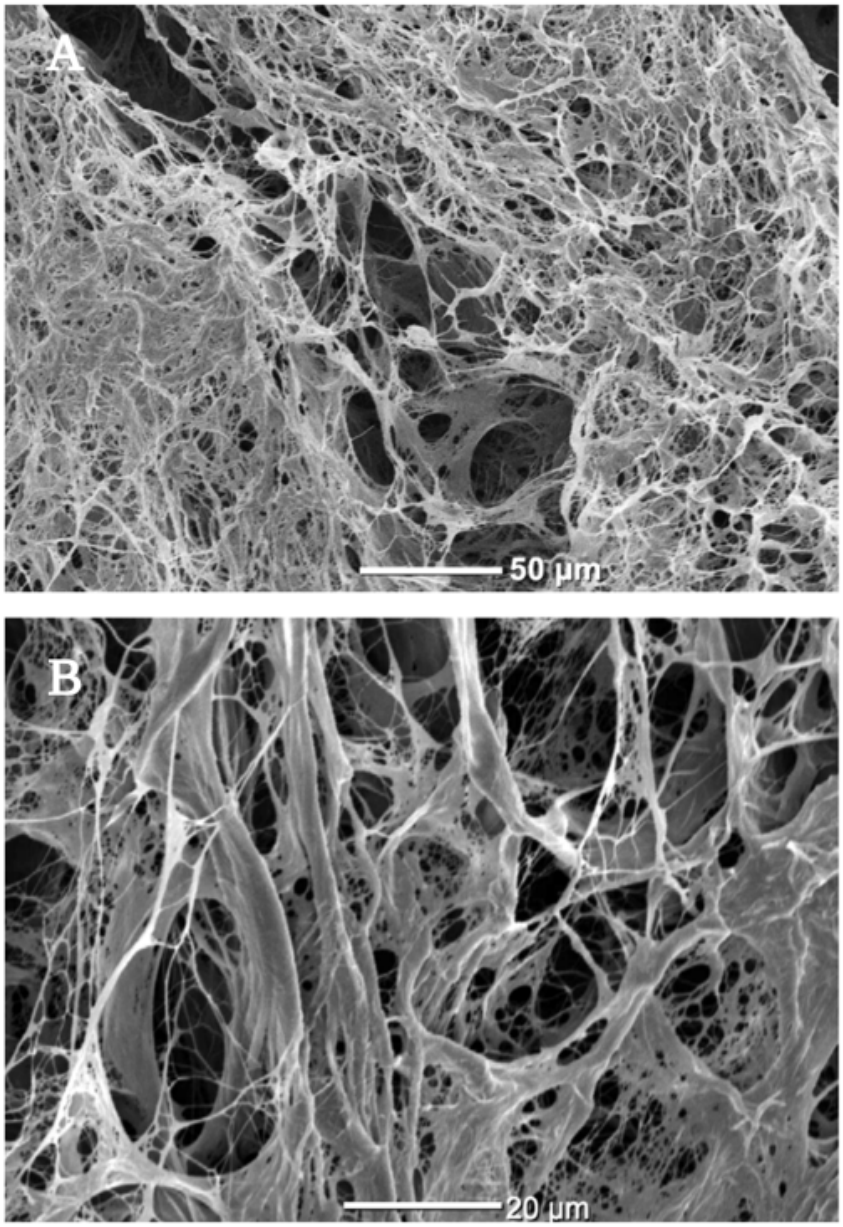

Figure 3.4: SEM images of the decellularized liver biomatrix at A) 400x and B) 1100x magnification

3.1.3 DNA Quantification Results

The DNA quantification results are shown below. The quantification showed a statistically significant decrease in DNA content between the fresh liver and decellularized liver biomatrix (**** $p<0.001$, t-test).

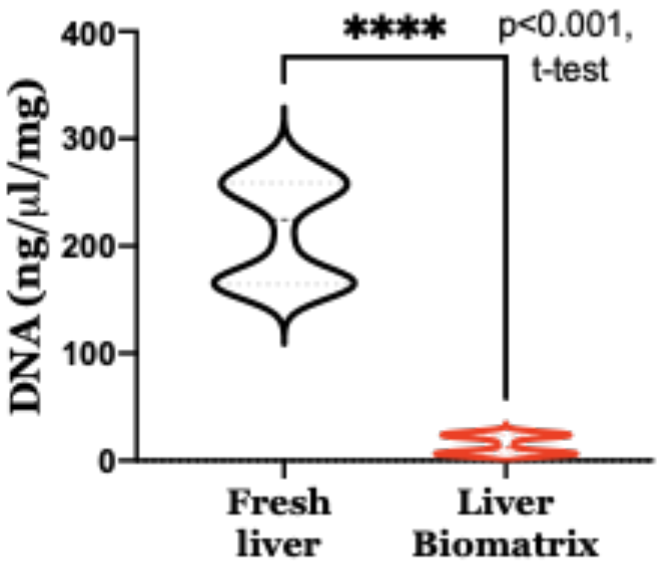

Figure 3.1: DNA content for fresh liver and decellularized liver biomatrix

3.2 OVCAR 3 Spheroid Results

The OVCAR 3 cell morphology and invasion into liver biomatrix scaffolds was compared for monospheroids and heterospheroids through the use of SEM and cell area quantification. Images of the OVCAR 3 spheroids prior to seeding onto the biomatrices are shown in Figure 3.6.

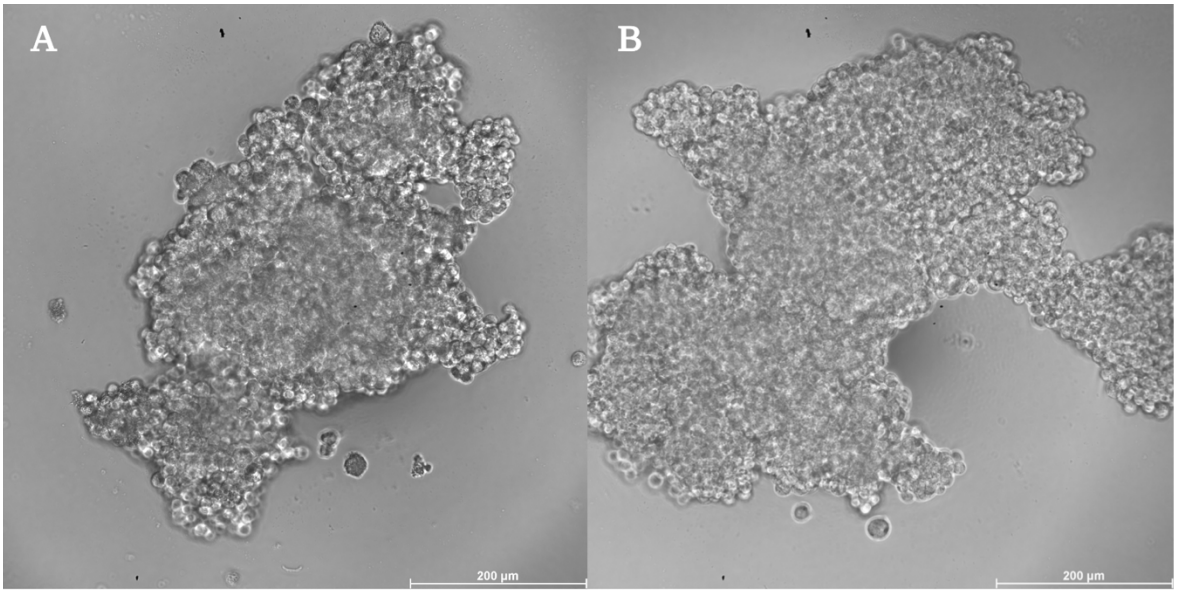

Figure 3.2: Images of A) OVCAR 3 monospheroids and B) OVCAR 3/macrophage heterospheroids were imaged with brightfield illumination

3.2.1 Scanning Electron Microscopy

3.2.1.1 OVCAR 3 Monospheriods

The liver biomatrices seeded with the OVCAR 3 monospheroids were imaged using SEM on days 3 and 7 of growth (shown in Figure 3.7). The proliferation of the spheroids over time is clearly demonstrated.

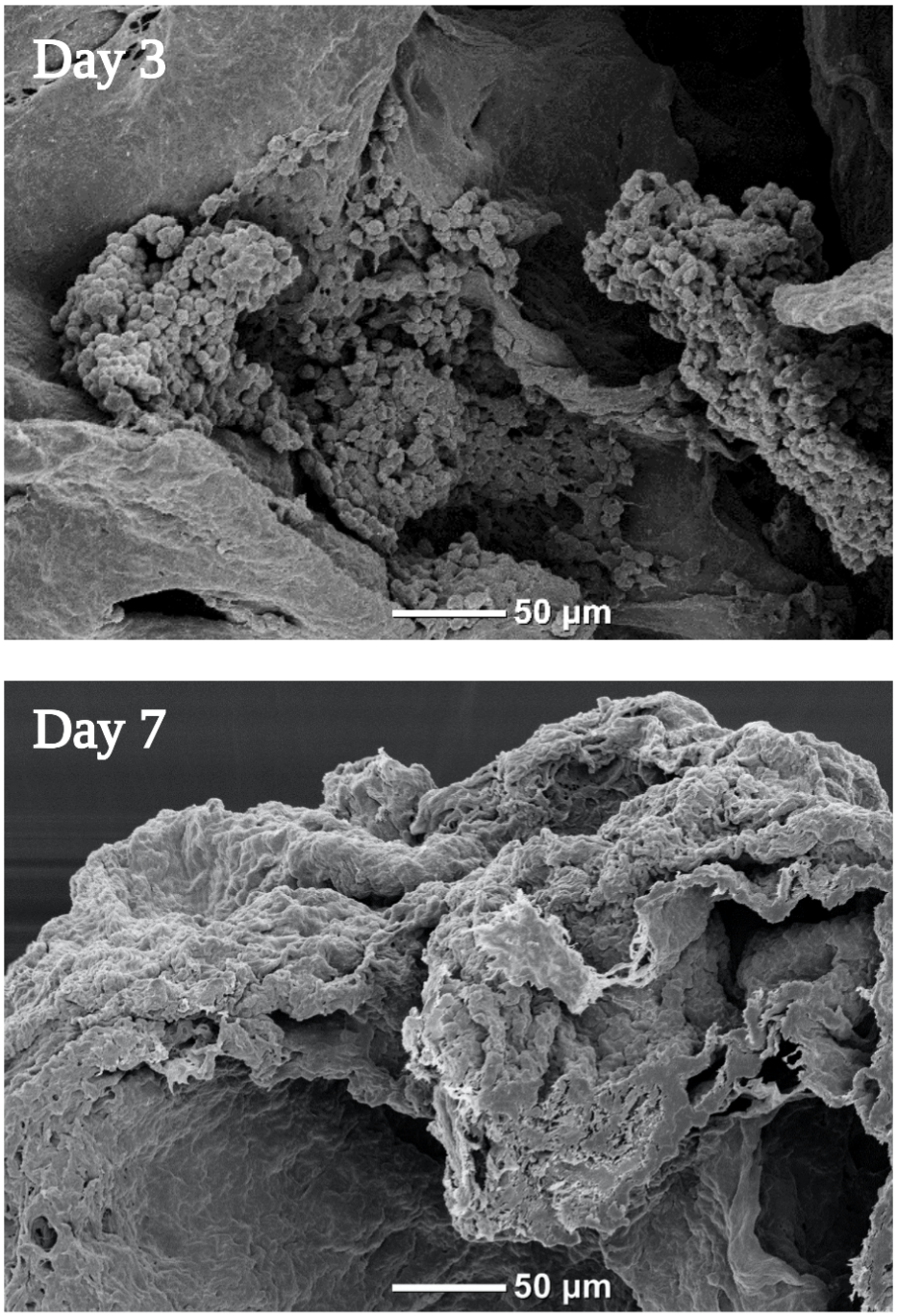

Figure 3.7: SEM images of the liver biomatrix seeded with OVCAR 3 monospheroids on days 3 and 7 of growth

3.2.1.2 OVCAR 3 and Macrophage Heterospheroids

The liver biomatrices seeded with the OVCAR 3/macrophage heterospheroids were imaged using SEM on days 3 and 7 of growth (shown in Figures 3.8). The proliferation of the spheroids over time can be seen.

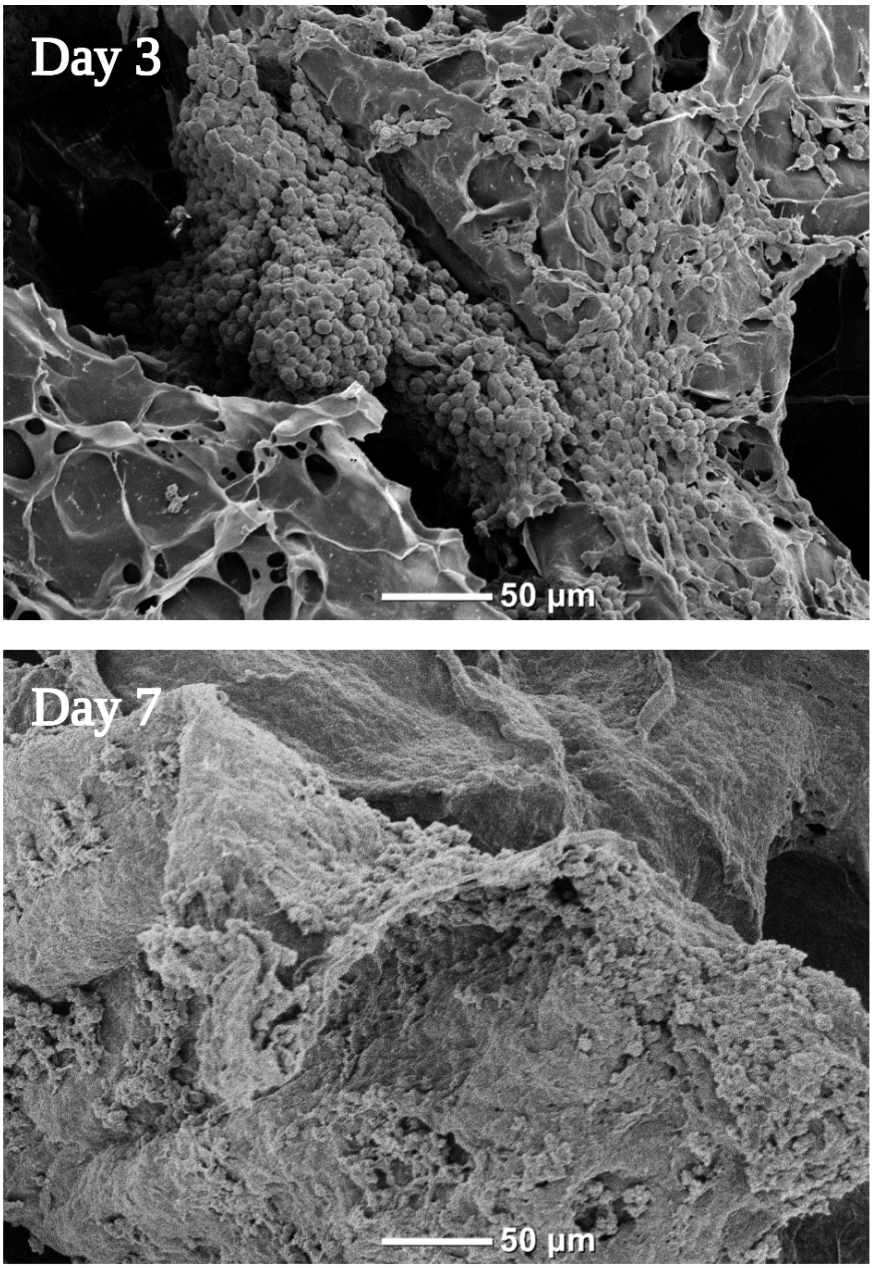

Figure 3.8: SEM images of the liver biomatrix showing OVCAR 3/macrophage heterospheroids invading the liver biomatrix structure on days 3 and 7 of growth

Comparing the SEM images from the monospheroids (Figure 3.7) and the heterospheroids (Figure 3.8), the morphology of the spheroids visibly changes with the addition of the macrophages. The monospheroids have a more spherical shape with regular, smooth boundaries. Meanwhile, the heterospheroids have rough, irregular boundaries and are less spherical in shape.

3.2.2 Cell Area Quantification

The proliferation of the OVCAR 3 spheroids with and without macrophages was quantified through the analysis of cell area in SEM images.

3.2.2.1 SEM Image Analysis

The percent area was calculated for the spheroids with and without macrophages. The results from the ImageJ analysis are shown in Tables 3.1 and 3.2 as well as Figure 3.9 below. There is an increase of 8.56% cell area on day 3 with the addition of macrophages to the spheroids. On day 7 of growth there is no statistical difference between the percent cell areas of the monospheroids versus the heterospheroids.

Table 3.1: Average percent cell area and standard deviation for days 3 and 7 of growth for the OVCAR 3 monospheroids

Monospheroids	Average % Cell Area	Standard Deviation
Day 3	26.19	5.49
Day 7	38.59	5.05

Table 3.2: Average percent cell area and standard deviation for days 3 and 7 of growth for the OVCAR 3/macrophage heterospheroids

Heterospheroids	Average % Cell Area	Standard Deviation
Day 3	34.75	14.39
Day 7	39.88	9.88

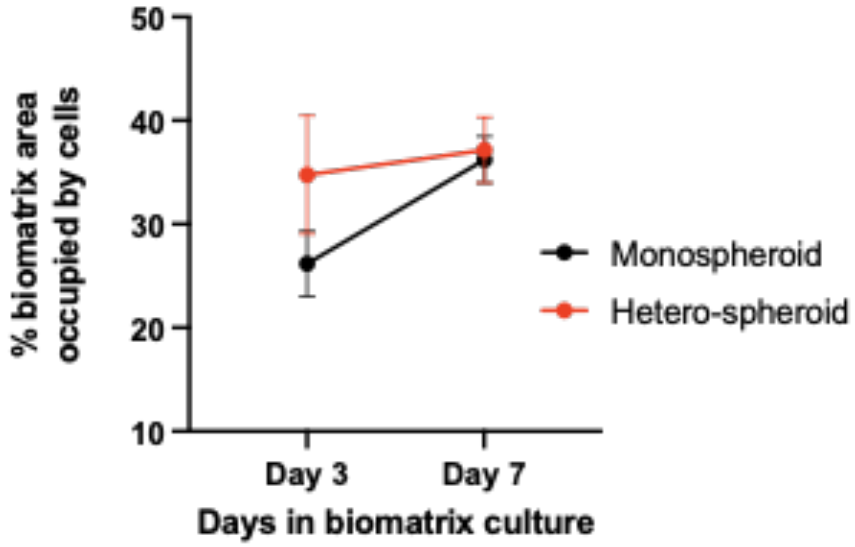

Figure 3.9: Invasion quantified by average percent cell area coverage of SEM images on days 3 and 7 of growth for OVCAR 3 monospheroids and OVCAR 3/macrophage heterospheroids

4. CONCLUSION

First, the decellularization of the liver biomatrix had to be characterized. Through the SEM and histology data, it was concluded that the liver biomatrix was decellularized effectively using the serial detergent rinse protocol established in lab. The SEM imaging both visually and quantitatively confirmed the absence of native cells in the biomatrix. DAPI staining showed no evidence of DNA content in the liver biomatrix. Due to these confirmational data, the liver biomatrix can be used as a decellularized 3D model of the hepatic TME.

Although the addition of macrophages did not result in a statistically significant increase in liver biomatrix invasion, visual indicators from SEM imaging suggest a trend towards increased invasion. Upon visual analysis of the SEM images, it was concluded that the addition of macrophages did have an effect on the morphology of the spheroids. The spheroids with macrophages had a different shape and irregular borders when compared to the spheroids with OVCAR 3 cells alone.

Our pilot studies established protocols to decellularize and characterize liver biomatrices for the study of metastatic cancer. Importantly, our studies demonstrate preliminary proof of concept for establishing metastatic nests from ovarian cancer monospheroids and ovarian cancer/macrophage heterospheroids. Decellularized liver biomatrices can be used as a 3D model for the hepatic TME, so nano-immunotherapies for OCLM can be tested more accurately with this model than with conventional metastasis models. In the future, this model can be used to investigate other forms of liver metastasis, such as colorectal cancer or breast cancer. Additionally, liver biomatrix use can be extended to other areas of research involving the hepatic microenvironment.

REFERENCES

[1] "Key Statistics for Ovarian Cancer." American Cancer Society. https://www.cancer.org/cancer/ovarian-cancer/about/key-statistics.html#references (accessed 2021).

[2] L. A. Torre *et al.*, "Ovarian cancer statistics, 2018," *CA: A Cancer Journal for Clinicians,* vol. 68, no. 4, pp. 284-296, 2018, doi: 10.3322/caac.21456.

[3] A. C. O'Neill *et al.*, "Patterns and Prognostic Importance of Hepatic Involvement in Patients with Serous Ovarian Cancer: A Single-Institution Experience with 244 Patients," *Radiology,* vol. 282, no. 1, pp. 160-170, Jan 2017, doi: 10.1148/radiol.2016152595.

[4] H. B. Frieboes, S. Raghavan, and B. Godin, "Modeling of Nanotherapy Response as a Function of the Tumor Microenvironment: Focus on Liver Metastasis," *Frontiers in Bioengineering and Biotechnology,* vol. 8, 2020, doi: 10.3389/fbioe.2020.01011.

[5] S. Raghavan, P. Mehta, Y. Xie, Y. L. Lei, and G. Mehta, "Ovarian cancer stem cells and macrophages reciprocally interact through the WNT pathway to promote pro-tumoral and malignant phenotypes in 3D engineered microenvironments," *Journal for ImmunoTherapy of Cancer,* vol. 7, no. 1, 2019, doi: 10.1186/s40425-019-0666-1.

[6] S. Raghavan *et al.*, "Formation of stable small cell number three-dimensional ovarian cancer spheroids using hanging drop arrays for preclinical drug sensitivity assays," *Gynecologic Oncology,* vol. 138, no. 1, pp. 181-189, 2015, doi: 10.1016/j.ygyno.2015.04.014.

[7] A. Albini, "Extracellular Matrix Invasion in Metastases and Angiogenesis: Commentary on the Matrigel “Chemoinvasion Assay”," *Cancer Research,* vol. 76, no. 16, pp. 4595-4597, 2016, doi: 10.1158/0008-5472.can-16-1971.

[8] A. Cho, V. M. Howell, and E. K. Colvin, "The Extracellular Matrix in Epithelial Ovarian Cancer – A Piece of a Puzzle," *Frontiers in Oncology,* vol. 5, 2015, doi: 10.3389/fonc.2015.00245.

[9] C. R. Justus, N. Leffler, M. Ruiz-Echevarria, and L. V. Yang, "In vitro Cell Migration and Invasion Assays," *Journal of Visualized Experiments,* no. 88, 2014, doi: 10.3791/51046.

[10] K. I. Hulkower and R. L. Herber, "Cell Migration and Invasion Assays as Tools for Drug Discovery," *Pharmaceutics,* vol. 3, no. 1, pp. 107-124, 2011, doi: 10.3390/pharmaceutics3010107.

[11] "Corning Matrigel Matrix." Corning. https://www.corning.com/worldwide/en/products/life-sciences/products/surfaces/matrigel-matrix.html (accessed 2021).

[12] C. A. Staton, M. W. R. Reed, and N. J. Brown, "A critical analysis of current in vitro and in vivo angiogenesis assays," *International Journal of Experimental Pathology,* vol. 90, no. 3, pp. 195-221, 2009, doi: 10.1111/j.1365-2613.2008.00633.x.

[13] D. M. S. Van Marion, U. M. Domanska, H. Timmer-Bosscha, and A. M. E. Walenkamp, "Studying cancer metastasis: Existing models, challenges and future perspectives," *Critical Reviews in Oncology/Hematology,* vol. 97, pp. 107-117, 2016, doi: 10.1016/j.critrevonc.2015.08.009.

[14] Lanuza *et al.*, "Optimizing the Decellularized Porcine Liver Scaffold Protocol," *Cells Tissues Organs,* pp. 1-10, 2020, doi: 10.1159/000510297.

[15] G. Rijal and W. Li, "A versatile 3D tissue matrix scaffold system for tumor modeling and drug screening," *Science Advances,* vol. 3, no. 9, p. e1700764, 2017, doi: 10.1126/sciadv.1700764.

[16] S. B. Yong, J. Y. Chung, Y. Song, J. Kim, S. Ra, and Y. H. Kim, "Non-viral nano-immunotherapeutics targeting tumor microenvironmental immune cells," *Biomaterials,* vol. 219, p. 119401, Oct 2019, doi: 10.1016/j.biomaterials.2019.119401.

[17] X. Li *et al.*, "Harnessing tumor-associated macrophages as aids for cancer immunotherapy," *Mol Cancer,* vol. 18, no. 1, p. 177, Dec 5 2019, doi: 10.1186/s12943-019-1102-3.

[18] G. R. Cindy Sampias. "H&E Staining Overview: A Guide to Best Practices." Leica Biosystems Richmond Inc. https://www.leicabiosystems.com/knowledge-pathway/he-staining-overview-a-guide-to-best-practices/ (accessed 2020).

[19] "DAPI stain." Thermo Fisher Scientific. https://www.thermofisher.com/us/en/home/life-science/cell-analysis/fluorophores/dapi-stain.html (accessed 2020).